Shock-Wave Propagation in a Sonoluminescing Gas Bubble

C. C. Wu and Paul H. Roberts
University of California at Los Angeles, Los Angeles, California 90024
(Received 28 December 1992)

The motion of the bubble radius and of the air trapped inside the bubble during sonoluminescence are determined self-consistently by coupling the solution of the Rayleigh-Plesset equation governing the bubble radius to the solution of Euler's equations for the motion of air in the bubble. Results are presented for three slightly different conditions of excitation, in two of which shocks are formed during the collapse of the bubble, and in which such high temperatures are attained that the air is ionized. Estimates are made of the duration and intensity of the light then radiated by the plasma.

PACS numbers: 47.55.Bx, 43.25.+y, 47.40.−x, 78.60.Mq

It has long been known that, when acoustic energy is focused on a bubble of air trapped in water, light may be emitted. Sound having a Mach number of order 10^{-5} is thus able to create photons with energies of several eV. This remarkable phenomenon is known as *sonoluminescence*. The sound waves generated by transducers are transmitted almost radially to focus on a bubble, the radius of which varies between a few tens of microns to a few tenths of a micron. They compress the air within it to high pressures, temperatures, and densities, during which time the light is emitted. Radiation, with a peak power of over 30 mW, occurs only during an interval of less than 50 ps within each cycle of the sound field, which has a period of a few tens of microseconds [1]. The simplest theories [2–4] suppose spherical symmetry and model the water as an (almost) incompressible fluid. The surface of the water acts like a piston that compresses and decompresses the air periodically.

The radius $R(t)$ of the bubble obeys [2–4] the *Rayleigh-Plesset equation:*

$$R\ddot{R}+\frac{3}{2}\dot{R}^2=\frac{1}{\rho_w}[p(R,t)-P_a(t)-P_0]+\frac{R}{\rho_w c_w}\frac{d}{dt}[p(R,t)-P_a(t)]-4\nu\frac{\dot{R}}{R}. \quad (1)$$

Here overdots denote differentiation with respect to time, ρ_w is the water density, p is the air pressure, P_0+P_a is the pressure in the water at great distances, P_0 is the ambient pressure, $P_a(t)=-P_a'\sin\omega_a t$ is the pressure of the acoustic field with a frequency of ω_a, ν is the kinematic viscosity of the water, and c_w is the speed of sound in water. The ambient radius of the bubble, R_0, is defined to be its size at NTP ($P_0=1$ atm and $T_0=300$ K).

Because of the enormous compressions in the bubble, Ref. [4] modeled the trapped air by a hard-core van der Waals equation of state, for which pressure p, specific volume V, temperature T, internal energy e, and entropy S are related by

$$p=\frac{\mathcal{R}T}{V-b},\quad e=c_v T=\frac{V-b}{\gamma-1}p,\qquad S=c_v\ln[p(V-b)^\gamma]+\text{const}, \quad (2)$$

where $\mathcal{R}$ is the gas constant, $c_v=\mathcal{R}/(\gamma-1)$ is the specific heat at constant volume, $\gamma=1.4$ is the ratio of specific heats, and $b=1/\rho_m$ is the van der Waals excluded volume. They assumed, as we shall, that $b=0.036$ liter/mole, so that $\rho_m\approx 794$ kg m^{-3} is the maximum possible density. The resulting $R(t)$ agrees with experiment much better than does the $R(t)$ for a perfect gas, $b=0$ [4].

To supply the $p(R,t)$ to close Eq. (1), Löfstedt, Barber, and Putterman [4] assume that the air moves adiabatically ($S=$const). Although the resulting $R(t)$ agrees well with experiment, the maximum temperature within the bubble ($\approx 10^4$ K) is much lower than the experimentally observed 10^5 K or greater [5]. They conjectured that this is due to the assumption of adiabaticity. They recommended that detailed calculations of the internal state of the bubble should be undertaken, including the generation of shock waves. In fact there have been two recent studies of such nonadiabatic models [6,7]. Moss *et al.* [6] have studied the compression of the air by a constant pressure applied to its boundary. They did not solve an equation of motion for $R(t)$ such as Eq. (1). Greenspan and Nadim [7] used Guderley's famous similarity solution [8] for radially moving sound waves to study the behavior of the shock launched by the bubble as it approaches and leaves the center of symmetry, O.

In what follows, we shall present solutions of the complete problem, i.e., that of the motion of the bubble surface, *and* the motion of a van der Waals gas within the bubble, including the generation and propagation of shocks. We therefore solve Eqs. (1) and (2) in conjunction with the gas flow equations in spherical symmetry,

$$\frac{\partial\rho}{\partial t}+\frac{1}{r^2}\frac{\partial}{\partial r}(\rho v r^2)=0, \quad (3a)$$

$$\frac{\partial}{\partial t}(\rho v)+\frac{1}{r^2}\frac{\partial}{\partial r}(\rho v^2 r^2)+\frac{\partial p}{\partial r}=0, \quad (3b)$$

$$\frac{\partial E}{\partial t}+\frac{1}{r^2}\frac{\partial}{\partial r}[(E+p)v r^2]=0, \quad (3c)$$

where r is distance from O, ρ is the gas density, $E=\frac{1}{2}\rho v^2+\rho e$ is the total energy density, and $v(r,t)$, the radial component of gas velocity, obeys $v(R,t)=\dot{R}$. We solved Eqs. (3a)–(3c) numerically using a Lax-Friedrich scheme and a moving grid of 800 points, with a temporal resolution of approximately 4×10^{-4} ps at times when the

radius of the bubble was near its minimum. The last grid point coincides with the boundary of the bubble. Our numerical scheme successfully recovered the similarity solution of Guderley [8] for an ideal gas.

We supposed that the bubble is transparent to radiation [9], and we *estimated* its optical luminosity $L(t)$ assuming that this is due to bremsstrahlung emitted from the air after it has been ionized by shock compression. For simplicity, we supposed that air consists of atoms of atomic weight 14.5 that are only singly ionized. We assumed that the ionization potential was (as for nitrogen) $\chi=14.5$ eV. To derive the degree q of ionization, we supposed that local thermodynamic equilibrium prevails, so that Saha's formula [10] applies: $q^2/(1-q)=2.4\times10^{21}T^{3/2}e^{-\chi/kT}/N$, where k is Boltzmann's constant and $N\approx4.16\times10^{25}\rho$ m^{-3} is the number density of atoms. We did not include modifications to the equations of state (2) arising from the ionization. We computed the radiative power emitted per unit volume from [11]: $P_{\rm Br}=1.57\times10^{-40}q^2N^2T^{1/2}$ W m^{-3}. (When Z electrons are ionized, this expression should be multiplied by Z^2.) The radiation generated in the bubble is absorbed by the surrounding water, except for that passing through a "window" of wavelengths greater than 200 nm. We integrated $P_{\rm Br}$ throughout the volume of the bubble, retaining *only* the fraction that passes through the window, and so obtained $L(t)$.

We present results for three cases (all for $b=1.26\times10^{-3}$ m^{3}kg^{-1} and $\nu=7\times10^{-5}$ m^{2}s^{-1}): (1) $P_a'=1.275$ atm, $R_0=4.5$ μm, $\omega_a/2\pi=26.5$ kHz; (2) $P_a'=1.5$ atm, $R_0=20$ μm, $\omega_a/2\pi=25$ kHz; (3) $P_a'=1.075$ atm, $R_0=10.5$ μm, $\omega_a/2\pi=26.5$ kHz.

Consider first case (1). Figure 1, which resembles closely those given in Ref. [4], shows $R(t)$ obtained by solving Eq. (1) under the assumption that the air moves adiabatically. The maximum bubble radius is $R_{\rm max}=37.09$ μm and is attained when $t=16.65$ μs. At that time, $\rho=0.0023$ kg m^{-3} and $p=14.36$ Pa. At the other extreme, the minimum bubble radius is $R_{\rm min}=0.59$ μm and is attained when $t=t_e\approx20.490$ μs. Then $\rho=574$ kg m^{-3}, $p=3.02\times10^9$ Pa, and $T=5695$ K. This integration provides a very useful comparison with results from the integration of the full system (1)-(3), i.e., from the nonadiabatic calculation.

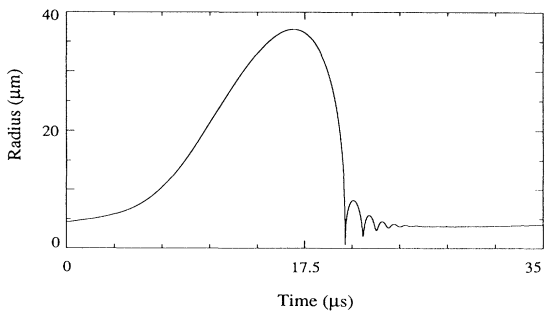

FIG. 1. Case (1): bubble radius vs time according to the adiabatic solution.

The nonadiabatic solutions scarcely differ from the adiabatic solution during the interval between $t=0$ and $t=16.65$ μs, so we used the adiabatic solution up to the moment of maximum radius and started integrating Eqs. (1)-(3) from $t=16.65$ μs with $\rho=0.0023$ kg m^{-3}, $p=14.36$ Pa, $v=0$, and $R=R_{\rm max}=37.09$ μm. From $t=16.65$ μs to the time when the bubble radius reaches $R_{\rm min}$, the solution $R(t)$ of the nonadiabatic system is close to that of the adiabatic system, but differences gradually magnify as $t=t_c$ is approached, especially in the air velocity v.

Figure 2 shows the time evolution for case (1) through a time interval $t_a<t<t_j$ of duration 0.417 ns spanning the instant $t=t_e\approx20.490474$ μs at which $R\approx R_{\rm min}$. There are four columns. Each column contains four panels, showing $\rho(r)$, $v(r)$, $p(r)$, and $T(r)$ for $0\le r\le R(t)$. The first column from the left shows the solution for $t=t_a=20.490257$ μs, $t_b=t_a+0.156$ ns, and $t_c=t_a+0.19864$ ns, during which the first shock-wave forms, at $r\sim0.3$ μm at $t\sim t_b$. The shock wave becomes stronger as it focuses at O, and this is shown by the solutions for $t=t_c$. At $t=t_c$, the shock speed is 2.5×10^4 m s^{-1}; the upstream values of density, velocity, and pressure are 101 kg m^{-3}, -18 m s^{-1}, and 5.5×10^7 Pa, respectively, and their downstream values are 407 kg m^{-3}, -1.9×10^4 m s^{-1}, and 6.1×10^{10} Pa, respectively. Near

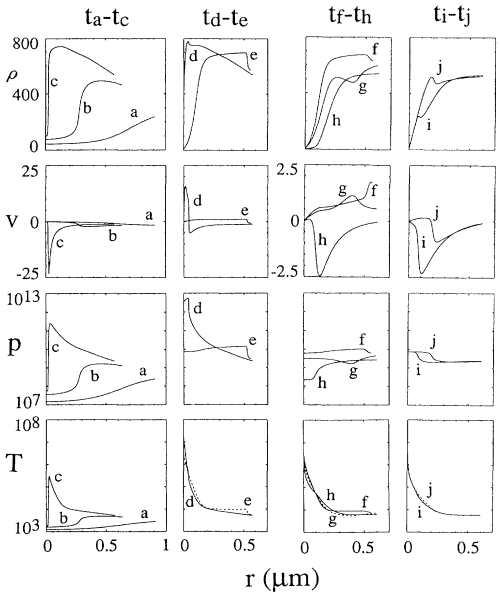

FIG. 2. Time evolution of case (1) from the nonadiabatic calculation. ρ is in kg m^{-3}, v in km s^{-1}, p in Pa, and T in K. Shown are solutions for (a) $t=t_a=20.490257$ μs; (b) $t_b=t_a+0.156$ ns; (c) $t_c=t_a+0.19864$ ns; (d) $t_d=t_a+0.19898$ ns; (e) $t_e=t_a+0.21641$ ns; (f) $t_f=t_a+0.22235$ ns; (g) $t_g=t_a+0.26172$ ns; (h) $t_h=t_a+0.377$ ns; (i) $t_i=t_a+0.396$ ns; and (j) $t_j=t_a+0.417$ ns.

the time at which the shock wave reaches $r=0$, the solution resembles Guderley's imploding shock-wave solution [8] for an ideal gas, but it is here modified by the van der Waals excluded volume. [A similarity solution exists [12] in which $R_S(t) \approx |t_c - t|^\alpha$ with $\alpha = 0.5$; for the perfect gas, $\alpha = 0.72$ [8].]

The second column of Fig. 2 shows the results for $t = t_d = t_a + 0.19898$ ns and $t_e = t_a + 0.21641$ ns. After focusing at O, a reflected shock wave forms, as the solutions for $t = t_d$ show. This reflected shock expands to meet the air moving towards the center. The result is again similar to that of Guderley's solution. But the reflected shock, which satisfies a jump relation modified by the van der Waals excluded volume, shows an increase of 7% in density, rather than the 230% increase of the Guderley solution. The shock wave moves outwards with an average speed of about 2.5×10^4 m s^{-1}. It strikes the boundary of the bubble about 0.018 ns after focusing; see the solutions for $t = t_e$.

The interaction of the shock wave and the bubble boundary may be thought of as a Riemann problem. Since the pressure inside the bubble boundary is about 10^{13} Pa and the external pressure is only about 10^5 Pa, the shock wave passes through the surface of the bubble and propagates outwards through the surrounding water. A rarefaction is created in the air which returns towards O, and the inward motion of the bubble boundary (the contact discontinuity) is reversed. Thus, at $t = t_e$, the bubble attains $R_{\min} = 0.55$ μm, which is 0.04 μm less than the value obtained from the adiabatic calculation. The solutions for $t = t_f = t_a + 0.22235$ ns in the next column of Fig. 2 confirm the formation of the inward rarefaction wave.

The results at $t = t_g = t_a + 0.26172$ ns and $t = t_h = t_a + 0.377$ ns show that, following the inward moving rarefaction wave, a second imploding shock wave forms which is much weaker than the first shock. After the second shock wave focuses, a second reflected shock emerges from O. This is seen in the last column of Fig. 2 for solutions at $t = t_i = t_a + 0.396$ ns and $t_j = t_a + 0.417$ ns.

Figure 3(a) shows the evolution of the bubble radius R and the shock-wave locations R_S during the time interval described above. Figures 3(b) and 3(c) show the density and the temperature on the shell where ρ is greatest as functions of t. As in Guderley's solution, the density jumps discontinuously at O when the shocks focus. In Guderley's solution, the density increases by a factor of 20.1 but in our case the factor is only about 7, because ρ must always be less than ρ_m. The temperature jumps discontinuously at the time of focusing. It becomes infinite in theory but, because of the finite resolution of the computation, finite in practice. The luminosity of the bubble is shown in Fig. 3(d). Consistent with the observations [5], a peak of about 30 mW was obtained, but its duration was only about 1.2 ps (as measured by the epochs at which half peak intensity is reached). It occurs about 0.1 ps after $t = t_d$, approximately 0.018 ns before

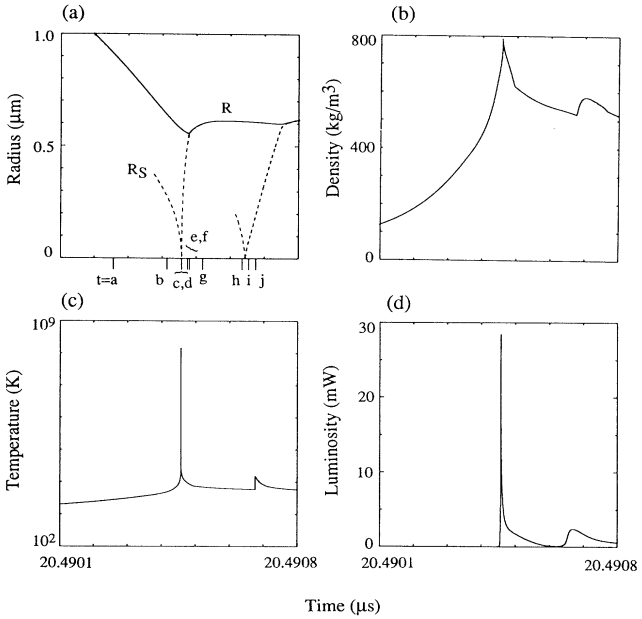

FIG. 3. Case (1): nonadiabatic solution. In (a), the bubble radius and the shock locations (dashed) are plotted as functions of time; the times $t_a - t_j$ employed in Fig. 2 are marked. In (b), (c), and (d), the maximum density, the temperature at maximum density, and the luminosity of the bubble are plotted as functions of time.

the bubble attains $R_{\min}$. During this peak, $q \approx 1$, i.e., the air is almost totally ionized. The major contribution to L arises from the vicinity of $r = 0.07$ μm where T is between 10^5 and 10^6 K. It is worth noting that the singularity that occurs at $(r,t) = (0,t_c)$ makes virtually no contribution to $L(t)$ and it is therefore hoped that the physical unreality of these infinities does not greatly influence the computed $L(t)$.

In summary, in case (1), the air within the bubble behaves very differently from the predictions of the adiabatic solution. A strong imploding shock front is formed during the collapse and, after its reflection from O, the temperature behind it becomes so large that the air ionizes, resulting in a plasma that emits a burst of light.

Consider next case (2). Figure 4 repeats for case (2) those shown in Fig. 3 for case (1). Very striking here is the much greater prominence of the second shock wave, which again behaves much as in Guderley's solution. Correspondingly, $L(t)$ exhibits a marked second peak, comparable with the first (≈ 3 mW); see Fig. 4(d). The times at which the first and second shock focus at O differ by approximately 1.2 ns, which is about 6 times longer than in case (1), probably because here $R_{\min} = 2.54$ μm is about 5 times larger than in case (1); also $R_{\max} \approx 98$ μm. It is remarkable that such apparently small changes in the conditions of excitation create such large differences in response. This sensitivity was also found for case (3): No shock is formed and the bubble behaves almost adiabatically.

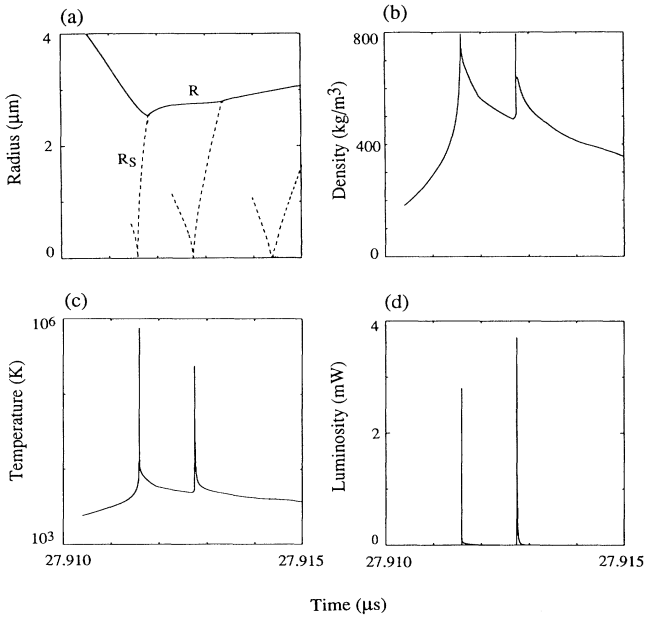

FIG. 4. Case (2): nonadiabatic solution. See caption to Fig. 3.

The continuum model studied here represents the first and most natural step in the theoretical study of sonoluminescence. We have excluded heat conduction within the bubble [13]. We have not attempted to incorporate an accurate equation of state for air. We have not allowed for deviations in the shape of the bubble from spherical symmetry.

We are grateful to Dr. S. J. Putterman for communicating the experimental and theoretical results of his group prior to their publication. One of us (C.C.W.) is supported by NSF Grant No. ATM-92-01662 and by NASA Grant No. NAGW-2848. Computing facilities were provided by the San Diego Supercomputer Center, which is sponsored by NSF.

[1] (a) D. F. Gaitan and L. A. Crum, J. Acoust. Soc. Am., Suppl. 1, **87**, S141 (1990); (b) B. P. Barber and S. J. Putterman, Nature (London) **352**, 318 (1991); (c) D. F. Gaitan, L. A. Crum, C. C. Church, and R. Roy, J. Acoust. Soc. Am. **91**, 3166 (1992); (d) R. Hiller, S. J. Putterman, and B. P. Barber, Phys. Rev. Lett. **69**, 1182 (1992); (e) B. P. Barber and S. J. Putterman, Phys. Rev. Lett. **69**, 3839 (1992).

[2] Lord Rayleigh, Philos. Mag. **34**, 94 (1917); M. Plesset, J. Appl. Mech. **16**, 277 (1949); J. B. Keller and M. Miksis, J. Acoust. Soc. Am. **68**, 628 (1980); A. Prosperetti and A. Lezzi, J. Fluid Mech. **168**, 457 (1986).

[3] C. Church, J. Acoust. Soc. Am., Suppl. 2, **89**, 1862 (1991); Barber and Putterman (Ref. [1(b)]).

[4] R. Löfstedt, B. P. Barber, and S. J. Putterman (private communication).

[5] Barber and Putterman (Ref. [1(e)]).

[6] W. C. Moss, J. W. White, R. A. Day, and D. B. Clarke, Lawrence Livermore National Laboratory Report No. UCRL-JC-110666 (to be published).

[7] H. P. Greenspan and A. Nadim (to be published).

[8] G. Guderley, Luftfahrtforsch. **19**, 302 (1942); see also L. D. Landau and E. M. Lifshitz, *Fluid Mechanics* (Pergamon, New York, 1987), 2nd ed.

[9] This represents a departure from the assumption of local thermodynamic equilibrium on which Eqs. (3) are based, but our estimate of the mean free path of photons of wave length 200 nm when air in the bubble ionizes is 8.6 μm (see [11]); this is large compared with the radius of the ionized region. Further, if the photons were in local thermodynamic equilibrium, the total peak luminosity from the bubble, ignoring absorption in the water, would be less than 2×10^{-4} W. The absence of spectral lines in the "window" of observation provides some support for our assumption that bremsstrahlung is the dominant process of light emission. According to Putterman (private communication), a bremmstrahlung spectrum fits the observations almost as convincingly as the black-body spectrum used by Barber and Putterman (Ref. [1(b)]).

[10] F. F. Chen, *Introduction to Plasma Physics* (Plenum, New York, 1974).

[11] S. Glasstone and R. H. Lovberg, *Controlled Thermonuclear Reactions* (van Nostrand, New York, 1960).

[12] S. J. Putterman (private communication).

[13] The thermal conductivity κ for T of interest is approximately proportional to $T^{1/2}$ and is therefore 180 times greater at 10^7 K than at NTP but, since the density at that time is 618 times greater (see above), the thermal diffusivity, $\kappa/\rho c_p$, is 3.4 times smaller, where c_p is the specific heat at constant pressure. The thermal diffusion time associated with a shock thickness of 0.1 μm is 1.2 ns, i.e., long compared with the interval of time during which shocks are present. We conclude that the neglect of thermal conduction in our calculations is not unreasonable.